Metal Matrix Composites

Subjects: Ergonomics

Contributor: Muhammad Arif Mahmood , Andrei C. Popescu , Ion N. Mihailescu

Metal matrix composites (MMCs) present extraordinary characteristics, including high wear resistance, excellent operational properties at elevated temperature, and better chemical inertness as compared to traditional alloys. These properties make them prospective candidates in the fields of aerospace, automotive, heavy goods vehicles, electrical, and biomedical industries. MMCs are challenging to process via traditional manufacturing techniques, requiring high cost and energy. The laser-melting deposition (LMD) has recently been used to manufacture MMCs via rapid prototyping, thus, solving these drawbacks. Besides the benefits mentioned above, the issues such as lower ultimate tensile strength, yield strength, weak bonding between matrix and reinforcements, and cracking are still prevalent in parts produced by LMD. In this article, a detailed analysis is made on the MMCs manufactured via LMD. An illustration is presented on the LMD working principle, its classification, and dependent and independent process parameters. Moreover, a brief comparison between the wire and powder-based LMDs has been summarized. Ex- and in-situ MMCs and their preparation techniques are discussed. Besides this, various matrices available for MMCs manufacturing, properties of MMCs after printing, possible complications and future research directions are reviewed and summarized.

3D printing | laser-melting deposition | wire- and powder-based laser-melting depositions | metal matrix composites | mechanical properties of metal matrix composites

1. Introduction

MMCs are usually composed of a minimum of two types of materials, a metal matrix and a dispersed phase of metal, ceramic, or polymer [1]. They can be classified into ex- and in-situ MMCs [2][3]. Figure 1a presents the ex-situ MMCs process, in which the reinforcements, usually particulates, are manufactured and mixed externally into the metal matrix. In such MMCs, the reinforced in the form of particulates are repeatedly splintered and cold-welded, thus, making them potential candidates for the SLS process. On the other hand, Figure 1b exhibits that in-situ MMCs are manufactured by a chemical reaction between the halide salts and metal matrix, which are thermodynamically more stable than ex-situ MMCs. In-situ MMCs show compatible, strong interfacial bonding and better mechanical properties as compared to ex-situ MMCs. Such MMCs are the potential candidates for SLM and LMD processes. There are various advantages of the MMCs, but potential difficulties, including gas entrapment, particle accruement, and micro- and macro-cracks, play obstacles to produce fully dense MMCs.

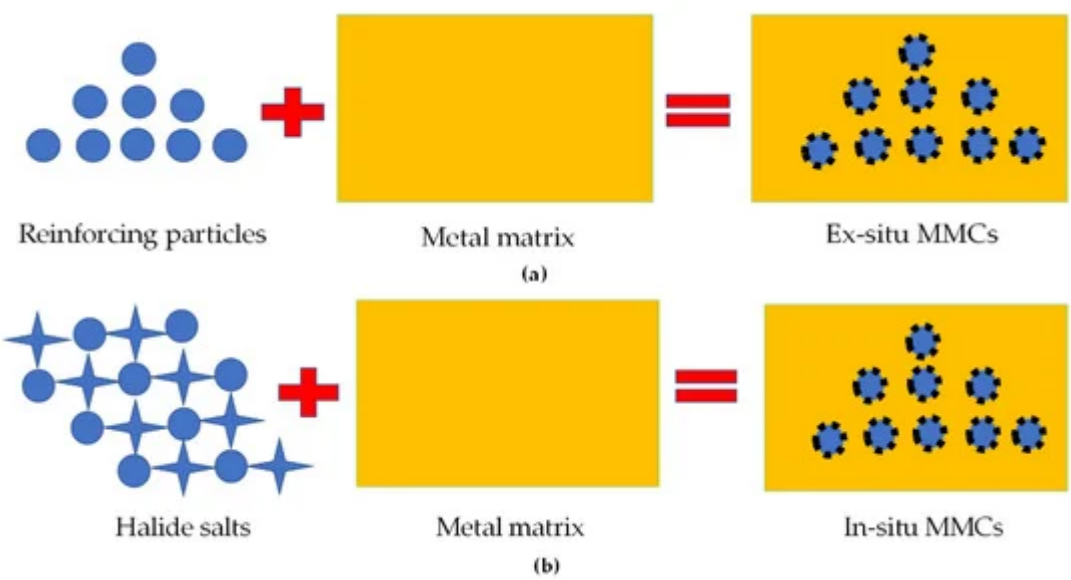

Figure 1. The graphical illustration of MMCs (**a**) ex-situ (**b**) in-situ; based on the data provided in Ref. [2][3].

2. MMCs Mixing Techniques

In the literature, various MMCs mixing techniques are available. The central perspective of these processing techniques is to achieve a standardized dispersal of the reinforcements within a matrix to achieve a defect-free microstructure. Table 1 collects the various MMCs mixing techniques.

Table 1. Mixing techniques for MMCs.

Technique Name and Description	Essential Features	References
• *Stir Casting* This technique involves the integration of ceramic particulate (reinforcements) into a liquid metal matrix by stirring mechanically and allowing the mixture to solidify.	(a) The dispersion of reinforcements is limited up to composites' 30 wt.%. (b) The reinforcement will not be homogeneous in the matrix if it is more than 30 wt.%. (c) The clustering of reinforcement is difficult to avoid. (d) Wettability is challenging to maintain.	[4][5][6][7][8]

Technique Name and Description	Essential Features	References
	(e) Segregation of reinforcing particles during floating takes place due to the density difference between the matrix and reinforcements. (f) Low-cost process.	
• *Rheocasting* In this process, the reinforcing particulates are mixed into the matrix, usually a metal. The given matrix is in between the solidus and liquidus temperature. The reinforcing particles are entrapped within the matrix, mechanically.	(a) An adequate bonding is achieved between the reinforcing particles and liquid matrix. (b) It results in better distribution of reinforcing particles, less porosity, improved wettability, and lower volume shrinkage. (c) It is a most reasonable method for fabricating the composites with discontinuous fibers or particulates. (d) It yields better distribution and integration of the reinforcing particles within the matrix as compared to the stir casting process.	[9][10]
• *Squeeze casting* In this technique, the pressure is applied and maintained until the molten metal solidifies. The applied pressure assists in grain refinement that ultimately enhances the mechanical properties of the final product.	(a) In this technique, the rapid solidification of the part is achieved. (b) Excellent strength and ductility are obtained due	[11][12][13][14]

Technique Name and Description	Essential Features	References
	to the rapid solidification process. (c) Gas porosity and shrinkage cavities are drastically reduced, resulting in excellent properties.	
• *Powder metallurgy* In this technique, a blending of fine powder particles, compacting into an anticipated form. Mostly, material heating is also involved.	(a) It is usually used for matrices with a high melting point. (b) It avoids segregation and brittle product formation. (c) It can produce complex shapes with satisfactory dimensional accuracy. (d) It yields minimum material loss. (e) Less secondary machining operations are needed. (f) The manufactured parts are relatively defect free. (g) It can incorporate a high-volume fraction of reinforcement.	[15][16]
• *Advanced shear technology* This process uses the melting-condition advanced shear technology technique. A sufficient quantity of shear stresses is applied to the particles, within the liquidus metal, to get over the cohesive force and the malleable strength of the given mixture. It consists of the following mixing steps:	(a) Near-net shaped MMCs are produced with homogeneously distributed reinforcements. (b) It can yield MMCs with suitable microstructures.	[17][18]

Technique Name and Description	Essential Features	References
Step I: Distributive mixing / *Step II: Dispersive mixing* It employs the conventional mechanical stirring to pre-mix the metal matrix with the reinforcing particles. The equipment is the same as stir casting. In this step, adequate shear stress is applied to overcome the average tensile strength of the agglomerated structures.	(c) The standardized dispersal of the reinforcement within the matrix is achieved. (d) Excellent mechanical properties are usually achieved, as compared to other techniques.	
• *Ultrasonic assisted casting* It is a well-known process to produce lightweight nano-metal matrix composites (NMMCs) with excellent reinforcement distribution. However, NMMCs present severe problems regarding the uniform dispersion in liquid metal that induces clustering. This drawback can be solved by integrating the ultrasonic system with the casting process.	(a) It can produce parts with better mechanical and machining properties as compared to any other casting process.	[11][19] [22]
• Friction stirring process It is a technique that can change the microstructure and mechanical properties through plastic deformation.	(a) It provides low production cost in a short time. (b) It needs a simple and inexpensive setup.	[20][21] [23]

literature,) + Al_2O_3 er feeding s, locally. %) within he tensile were pre- and lower elongation as compared to the monolithic matrix alloys at 873 K. The UTS decreased from 625 to 342 MPa as the temperature increased from 873 to 973 K. In contrast, the elongation of the MMCs increased from 7% to 18%.

Liu et al. [24] manufactured titanium matrix composites (TiC + TA15) by the LMD process. Initially, the TiC + TA15 in powder form was mixed with an acetone solution, and then the slurry was dried in an electric oven up to 393 K for two hours to eliminate the acetone solvent. The results are shown in Figure 2, which indicates that the specimen containing TiC (5 vol.%) presented better yield strength (YS) and UTS. In contrast, the tensile properties of the composites declined with the further increment of TiC (10 and 15 vol.%). The declination in the UTS of the composites is accredited to the premature failure of the TiC reinforcements. It can also be seen that pure TA15 presented better elongation (%) as compared to the composite ones.

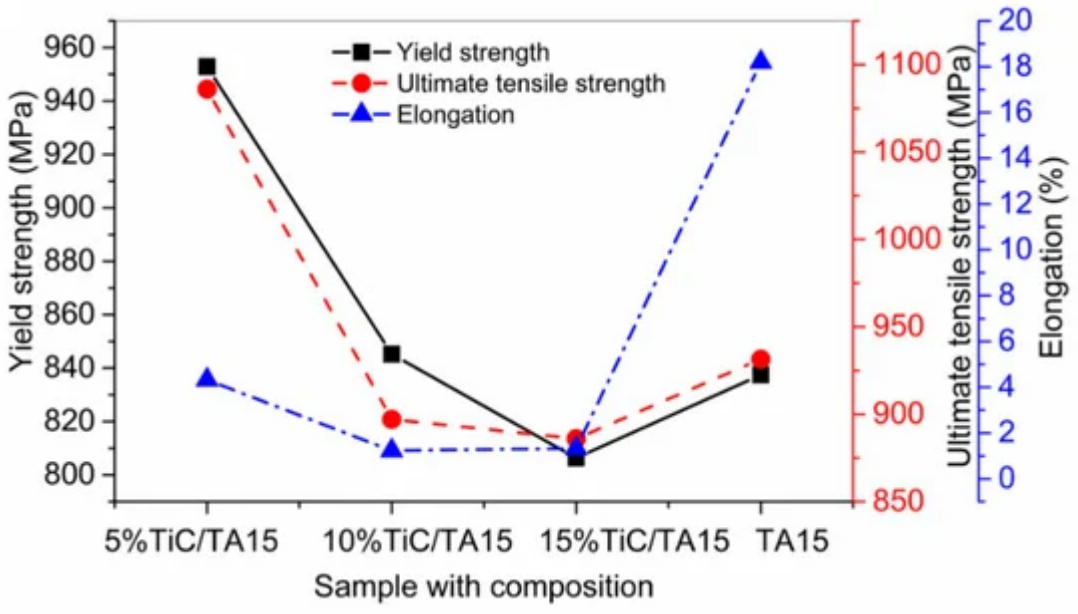

Figure 2. TiC + TA15 composites mechanical characteristics, including yield strength, ultimate tensile strength, and elongation; based on the data provided in Ref. [24].

Cooper et al. [25] manufactured MMCs with the addition of Al_2O_3 + SiC + TiC (5 wt.%) in the Inconel 625 matrix by the LMD process. A ball mill was used to mix the powders, at a speed of 150 rpm for one hour, until the powders appeared well-mixed visually. On the one hand, the material hardness increased up to 130%. On the other hand, the number of pores and cracks increased with the addition of SiC. In contrast, no appreciable effect upon material's hardness was found with the addition of Al_2O_3.

3. Metal Matrix Composites (MMCs) Deposited by Wire and Powder Particles Feedstock

The LMD process can be further classified based upon the type of feedstock material. Figure 3 presents the two deposition techniques derived from the LMD process. In Figure 3a, the powder is fed coaxially along the laser beam while the lateral wire feeding into the melt pool can be observed in Figure 3b [26].

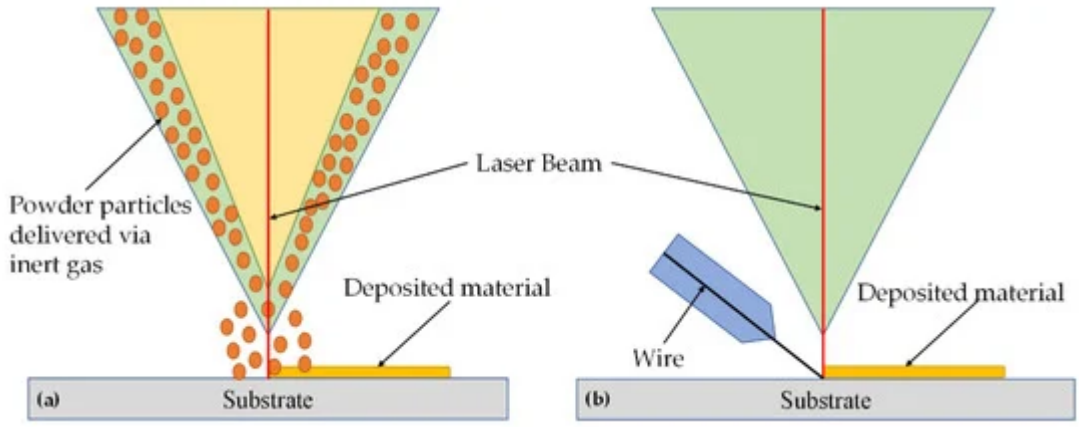

Figure 3. The LMD process: (**a**) coaxial powder feeding and (**b**) lateral wire feeding; based on the data provided in Ref. [26].

Processes, as mentioned earlier, own some pros and cons, which are summarized in Table 2 [27][28][29][30][31].

Table 2. Comparison between the powder and wire-based LMDs.

Powder-Based LMD		Wire-Based LMD		References
Pros	***Cons***	***Pros***	***Cons***	
• Various materials can be processed. • Complex shapes can be built. • Functionally graded materials are manufactured.	• It results in high porosity percentage. • Material cost is high. • Deposition efficiency is less. • Powder particles lead to serious health issues.	• Material waste is lesser as compared to powder-based LMD. • The deposition rate is high. • The feedstock is less expensive than powder-based LMD.	• The material's feed rate cannot be controlled. • It requires high energy. • The dilution rate, in the substrate, of the deposited material is higher than powder-based LMD.	[27][28][29][30][31]

The pros and cons of combined powder- and wire-based LMDs are presented in Table 3 [26].

Table 3. Integration of powder- and wire-based LMDs.

Powder + Wire-Based LMDs		References
Pros	***Cons***	
• Higher deposition efficiency. • Higher energy valorization. • Optimum resource consumption.	• Difficulty in the integration of powder- and wired-based LMDs. • Staff training, evaluation and testing of produced parts will cause a cost increment.	[26]

Farayibi et al. [32] investigated the LMD of Ti6Al4V (wire) + tungsten carbide (WC), in powder form, fed concurrently into the melt pool generated on a Ti6Al4V substrate via the laser beam. The WC particulates participated as the strengthening agent within Ti6Al4V, thus, improving the deposited MMCs' hardness and wear resistance. Figure 4 shows the microhardness of the deposited material, in which the powder flow was increased (10–40 g/m), while the wire feed rate kept constant (800 mm/min). It can be analyzed that with the increment in powder flow, the hardness of the deposited MMCs rises significantly (600–1000 HV).

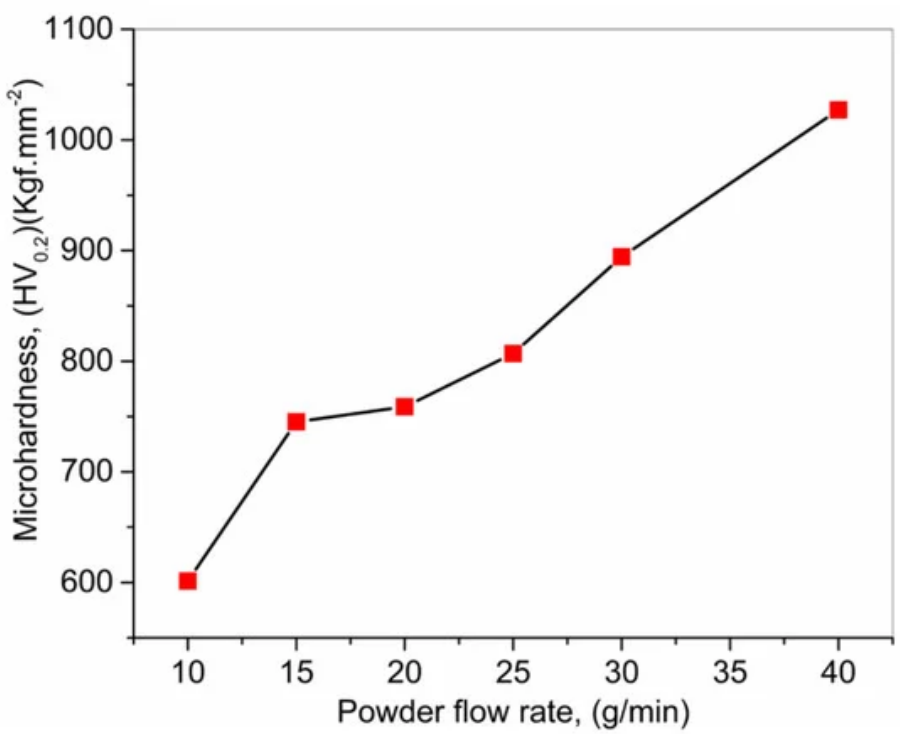

Figure 4. Effect of WC powder flow rate on microhardness; based on the data provided in Ref. [32].

Farayibi et al. [33] developed a new MMC using Ti6Al4V + titanium diboride in the powder form via a satelliting method. The resulted mixture consisted of large Ti6Al4V particles, enclosed within finer needle-shaped TiB structures, presented an improved hardness. The microstructural characterization exposed that the composite consisted of TiB eutectic precipitates in an α+β-Ti-matrix. They contained the incompletely melted Ti6Al4V + TiB_2 particulates. The satelliting of TiB_2 particles onto Ti6Al4V surfaces notably enhanced the dispersion of the composite, which was characterized by the arbitrarily oriented and uniformly distributed TiB needles within the microstructure. The composites' hardness, when fabricated by this technique, was in between 440 to 480 HV.

3. Different Laser Sources for In-Situ MMCs Syntheses by LMD

Various studies to manufacture MMCs by a unique laser source have been proposed. Ramakrishnana and Dinda [34] manufactured MMCs using Al (82 wt.%) + W (18 wt.%) via the LMD technique. A laser beam (diode laser Laserline LDM 2000-40, 978 nm) of 900 W, in combination with three scanning speeds (1.5, 6, and 12 mm/s), was

used for the MMCs fabrication. The hardness of the developed MMCs increased up to 50% in comparison with pure aluminum. A finer microstructure was found at 12 mm/s scanning speed as compared to 1.5 and 6 mm/s scanning speeds. Zhenglong et al. [35] prepared TiB_2 (particulate) + AA7075 (matrix) MMCs using the LMD technique. A laser beam (IPG fiber laser, YLS-5000) with 800 W and 10 mm/m scanning speed was used in the process. The results exhibited that the grain dimensions decreased after adding TiB_2 due to heterogeneous nucleation. In comparison to the unreinforced AA7075 sample, TiB_2 + AA7075 MMCs showed an elevated hardness. The hardness of the MMC with TiB_2 (4 wt.%) was found to be 127.8 HV, while the grain size was reduced up to 16.8 µm.

Li et al. [36] designed and fabricated novel MMCs using α-Fe, vanadium (V), victorium (VC), and chromium carbides (Cr_7C_3, $Cr_{23}C_6$) via the LMD process. The V was used in 9, 12, and 15% (wt.%), respectively. For fabrication, a ytterbium laser source with 2.2 kW and 8 mm/s scanning speed was used. The results indicated that the VC particles provided adequate space for the heterogeneous nucleation of α-Fe and $Cr_{23}C_6$, during the solidification of the molten material, which resulted in refined grain structures. The microhardness of the three specimens was in the range of 521–603 HV. The sample having V with 12 (wt.%), resulted in the lowest wear rate (5.011×10^{-6} mm^3/Nm) among all the tested samples.

4. Matrices for MMCS

4.1. Titanium-Based MMCs (TMCs)

Titanium alloys have various aerospace, marine, biomedical, structural and industrial applications. They owe excellent strength to weight ratio, malleability, formability, deterioration resistance, and biological compatibility characteristics. However, these alloys yield reduced hardness and wear attributes. A suitable way to increase the hardness and tribological characteristics of Ti-alloys is to mix the Ti-matrix with tough precipitates to achieve Ti-based composites (TMCs). These can be classified into two sub-categories based on the type of reinforcement: (i) continuous reinforced TMCs (ii) discontinuous (particles) reinforced TMCs [37][38][39]. Table 4 summarizes the continuous and discontinuous TMCs formation techniques regarding illustration, advantages, and disadvantages.

Table 4. Continuous and discontinuous TMCs formation techniques.

Continuous Reinforced TMCs Formation Techniques			
Technique and illustration	*Pros*	*Cons*	References
• Lay-up methodology • It involves alternating depositions: Woven fiber rugs + 0.90–0.16 mm thick Ti-alloy foils.	• It can accommodate high and more extended fiber contents in comparison with the spray technique.	• It uses excessive foil and fibers. • It results in homogenous fiber dispersion and fabrication difficulties.	[40]

Continuous Reinforced TMCs Formation Techniques			
	• The usage of low-temperature resins results in low tooling cost.		
• Induction plasma deposition • It uses an inductive high-frequency plasma to melt and sprinkle the fine-grained microstructures of Ti-matrix onto a wound fiber drum.	• The fiber spacing is highly maintained. • Any metal matrix, which can be transformed into powder, is used in this process.	• A strict composition control is needed.	[41]
• Physical vapor accumulation • It comprises the build-up of matrix onto a solitary fiber layer via vaporization of a metal matrix using an electron beam or magnetron sputtering.	• The distribution of fiber is excellent. • The complex shapes can be produced.	• The production cost is high. • Specialized skills are required. • It is relatively a slow process.	[42]
• Tape casting • It contains slurry formation; then, the reinforcements are coated with slurry and cut into desired shapes.	• It requires consolidation steps to obtain homogenous material, which increases the production cost.	• The contamination control is difficult due to titanium reactive nature and the presence of polymeric additives.	[43]
Discontinuous Reinforced TMCs Formation Techniques			
• Powder metallurgy • It involves the homogenous mixing of various powders/halide salts to produce ex-and in-situ TMCs	• A most suitable technique to produce TMCs. • The production cost is reasonable.	• Homogenous mixing is a critical step. • Sometimes the surface coating is needed to reach homogenous properties.	[44][45]

Continuous Reinforced TMCs Formation Techniques			
	• The production rate is high.	• The selection of reinforcement presents a critical role in TMCs' final features.	
• Rapid solidification process • In this process, "atomization" technique is used; reinforcements are added into the molten material. It is mostly used for in-situ TMCs.	• It is a straightforward technique. • The investment cost is lesser than the other techniques.	• It requires high heat as an input. • A difference in the reinforcements and matrix densities results in the MMCs with non-uniform properties. • The processing temperature can affect the size and scale of particulates.	[46][47][48]

ion. They Ti-alloys. Different particulates have been selected for reinforcement so far such as TiB_2, TiN, B_4C, ZrC [49][39], nano-SiC [50], TiB, TiC [51][52], Al_2O_3 [53], and Si_3N_4, which were found unstable due to the formation of titanium silicide and carbon nanotubes [54][55][56]. For the continuous fibers, TMCs using boron reinforcing fibers (coated with silicon carbide) were produced; however, these fibers are expensive as compared to the other fibers, which leads to discontinuation of TiB fibers [39][57][58]. Besides this, various researches have been carried out using SiC [59][60][61][62][63], carbon [39][64][65], SCS-6 and Sigma [66][67] reinforced fibers.

Figure 5a displays the mechanical and physical properties of various discontinuous TMCs. It can be seen that the TiB and graphene present the least and highest melting point, respectively, as compared to the other discontinuous reinforcements (DRFs). It means that a low amount of laser energy will be needed to melt down the TiB. In contrast, an opposite behavior can be observed for graphene. Moreover, La_2O_3 presents the highest density, while graphene possesses the least density value. To the best of our knowledge, the elastic modulus of TiB and La_2O_3 containing MMCs are not reported in the literature, which identifies the potential area for future research. The B_4C, SiC, TiB_2, TiC, and TiN have almost the same elastic moduli; but, the carbon nanotubes (CNTs) and graphene present the highest elastic moduli as compared to the rest of DRFs. Similarly, the La_2O_3 has the highest thermal expansion coefficient as compared to the rest of DRFs. Figure 5b shows a comparison of various continuous reinforcements (CRFs) regarding their diameter and ultimate tensile strength (UTS). The two major types of CRFs, including SiC and Al_2O_3, have been presented. The majority of the CRFs such as SM 1140+, trimarc, SCS-ultra, and SM-6 belong to the SiC category, while sapphire belongs to the Al_2O_3 type. The output explains that SCS-ultra, with a diameter of 140 µm, shows the maximum UTS. In contrast, for the rest of the CRFs, a compromise should be reached between the particulate size and UTS. By keeping in view the trend presented in the Figure 5, one can

conclude that the proper selection of DRFs and CRFs has to be made based on the specific requirements, and a compromise should be made between the thermal and physical properties [39].

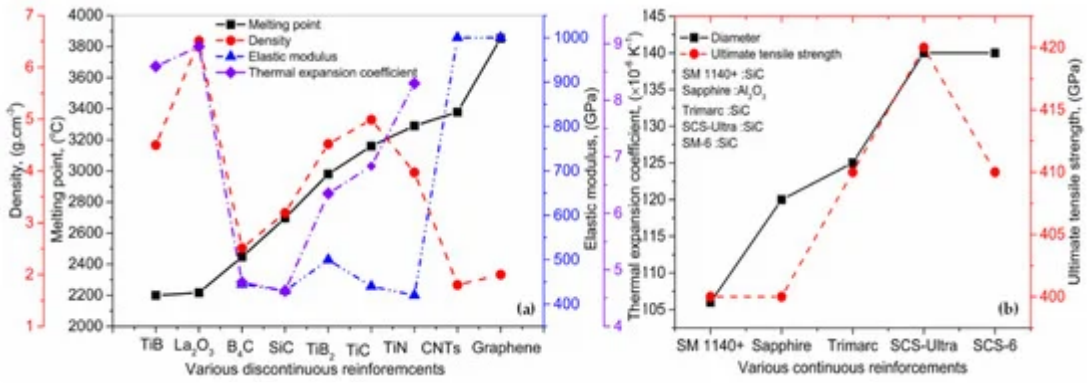

Figure 5. Properties of various TMCs (**a**) discontinuous and (**b**) continuous reinforcements; based on the data provided in Ref. [39].

4.2. Nickel-Based MMCs (NMCs)

Ceramic reinforced nickel matrix composites, also known as NMCs, usually possess high fatigue and corrosion resistance with better hardness and wear resistance properties as compared to the simple nickel matrix. They are considered to be prospective materials in aerospace, biological, and petrochemical manufacturing due to above-mentioned properties. TiC strengthened NMCs via LMD were produced by Hong et al. [68]. They found that the existence of TiC was beneficial to refine grain size, from 34.1 µm to 27.2 µm. Moreover, the results displayed that the high energy can lead to an effective Marangoni convection confined by the melt pool, which induces refined and normalized spreading of TiC reinforcements. Thus, resulting in improved wear resistance and malleability. Furthermore, an increment in the thermal energy input per unit length resulted in uneven columnar dendrites formation, declining the wear and tensile properties of NMCs. Li et al. [69] produced Ni + TiC NMCs by LMD. A total of three TiC compositions, including 20, 40, and 60 (vol.%), were selected. The influence of TiC vol.% on phase transformation, microstructure evolution, hardness, and wear resistance, was analyzed. The analyses exhibited that the composites consisted of TiC + Ni phases, demonstrating that TiC was produced through in-situ reaction. Moreover, TiC particulate size increased from 3 to 10 µm, when the TiC (vol.%) was enhanced from 20 to 60%. In addition, the hardness was improved from 365.6 $HV_{0.3}$ to 1897.6 $HV_{0.3}$, while the value of wear resistance changed from 20 to 6×10^{-3} g.

4.3. Other Metal Matrix Composites

In the LMD process, the rapid heating and solidification lead to the warpage, delamination, and cracks. Li et al. [70] carried out a study on the usage of invar. The experimental results showed that TiC reinforced invar, with the 64 wt.% Fe and 36 wt.% Ni composition, has a low thermal expansion coefficient, improved rigidity, and YS. Xiong et al. and Picas et al. [71][72][73] manufactured WC + Co using LENS. An improved microstructure, wear resistance, and mechanical properties were found with the addition of WC in Co. Choi and Maumder [74] reported a study on the manufacturing of Fe + Cr + C + W MMCs via the DMD, thereby, producing an innovative wear-resistant

material. The results explained that the conformation and volume proportion of carbides could easily be handled by regulating the pre-heating temperature, input power density, and scanning speed. The matrix participation was carried out by M_6C and $M_{23}C_6$ type carbides; the rhombus-shaped M_6C carbides showed better tribological properties. Zhong et al. [75] synthesized the Ni-Al intermetallic layers and TiC (particulates) MMCs by laser cladding. The powder particles were added coaxially. The printed layers were cracks free and metallurgically bond to the substrate. The microstructure of the layers was mainly composed of β-Ni-Al phase and a few γ-phases. Moreover, un-melted dispersive fine precipitates of TiC particles and refined β-Ni-Al phase matrix were found in the composites. The hardness test shows that the microhardness for Ni-Al intermetallic layers was equal to 355 $HV_{0.1}$, and 538 $HV_{0.1}$ for Ni-Al+ TiC matrix composites.

5. Properties of MMCs

MMCs present remarkable characteristics, which makes them applicable in the fields of aerospace, automotive, heavy goods vehicles, electrical, and biomedical [76]. Few properties of MMCs are reviewed below.

5.1. Mechanical Properties: Hardness, Ultimate Tensile Strength (UTS), Yield Strength (YS), Elongation, and Wear

MMCs present superior properties including hardness, YS, and UTS in comparison to the base alloys. Li et al. manufactured MMCs through the LMD by feeding the WC powder particulates along with titanium wire into the melt pool generated by the laser beam. Major process parameters, including wire feeding rate, powder flow, and the laser power were used in the analyses. The microhardness of the MMCs was 500 $HV_{0.2}$, which is much higher than the titanium alloys (320 $HV_{0.2}$). It indicates that the presence of the WC + TiC phases within the printed layer improved the hardness and abrasive resistance. Bi et al. [77] carried out the deposition of inconel 625 + TiC nano-powders using the LMD. The mechanical properties were investigated. Three different compositions of TiC + inconel 625, including 0.25/99.75, 0.50/99.50 and 1.00/99.00 (wt.%), were synthesized. The hardness, UTS, YS, and elongation are shown in Figure 6a. It can be seen that the hardness, UTS, and YS increased proportionally with the increment in the quantity of TiC particulates (wt.%). However, elongation presented random behavior with the increment in TiC particulates (wt.%). The maximum elongation was exhibited by 0.50/99.50 composition. Gopagoni et al. [78] processed Ni (80 wt.%) + Ti (10 wt.%) + C (10 wt.%) MMCs via LENS technique. The manufactured MMCs showed the eutectic TiC and FCC-TiC structures. The tribological and mechanical analyses were conducted. The stationary friction coefficient was found equal to 0.50, inferior to pure Ni. Moreover, the hardness increased substantially up to 370 VHN, proving them a potential candidate for surface engineering operations. Crack-free functionally graded MMCs composed of TiC particulates + Ti6Al4V were manufactured by Wang et al. [79] using LMD. A volume fraction of TiC in between 0–30 (% wt.) was used to analyze the effect of TiC (vol.%) on the microstructure and mechanical characteristics of MMCs. They found that the hardness gradually increased with the increment in TiC (vol.%), which can be attributed to the presence of eutectic + TiC phases. When TiC increased up to 5 (vol.%), the tensile strength enhanced by 12.3% as compared to the Ti6Al4V alloy. Nevertheless, the tensile strength and elongation of the produced MMCs decline as the volume fraction of TiC

surpass by 5%. It can be explained that the number of stiff un-melted TiC particulates, amount and dimension of dendritic TiC phases raised with the increment in TiC. These results are presented in Figure 6b.

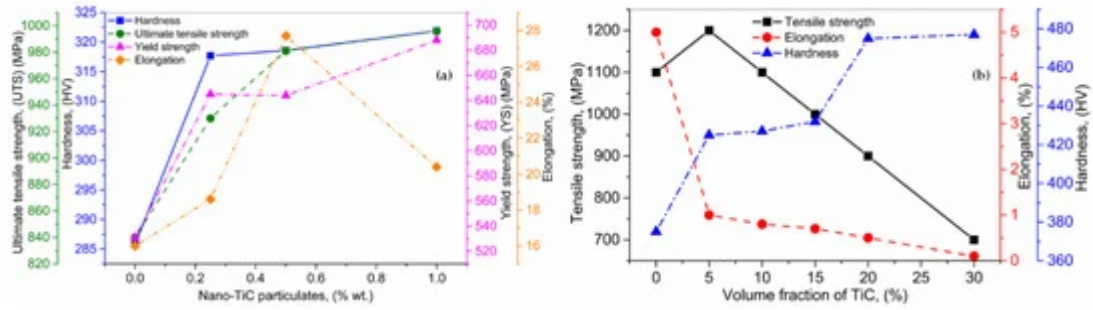

Figure 6. (**a**) Influence of Nano-TiC particulates on the hardness, ultimate tensile strength, yield strength, and elongation, and (**b**) the consequence of TiC (vol.%) on Tensile strength, elongation, and hardness; based on the data provided in Ref. [77][79].

Hong et al. [80] used the LMD to manufacture inconel 718 + TiC MMCs. The influence of the laser energy over the unit length (80–160 kJ/m) on the microstructures and hardness, was analyzed. The TiC experienced a tremendous transformation as the laser energy density increased from 80 to 120 kJ/m. The comparatively coarse polyhedral TiC particulates resulted when the laser energy was up to 100 kJ/m. As the laser energy increased beyond 100 kJ/m, completely liquified smooth TiC particulates were produced. Furthermore, when the laser energy increased beyond 160 kJ/m, the TiC particulates were significantly refined. However, a direct relationship was observed between laser energy input and microhardness for the produced MMCs, as given in Figure 7a. Sateesh et al. [81] manufactured MMCs using pre-heated nickel phosphide coated with SiC reinforced particles via the LMD process, under inert nitrogen atmosphere. An inclination in the hardness, UTS, YS, and elongation was observed with the increment in SiC (wt.%). These properties decline dramatically beyond 3 (wt.%) addition of SiC. For a given laser scanning speed and power, the increment in SiC (wt.%) resulted in excessive un-melted SiC particles, leading to the declination of hardness, UTS, YS, and elongation, as shown in Figure 7b.

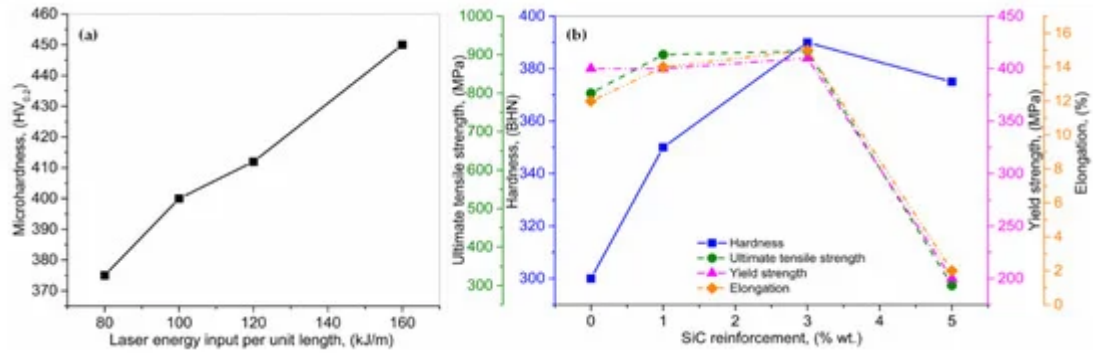

Figure 7. (**a**) Analyses of laser energy input over the unit length on microhardness, and (**b**) influence of SiC reinforcement (wt.%) on hardness, ultimate tensile and yield strengths, and elongation; based on the data provided in Ref. [80][81].

Zhang et al. [82] used the LMD to manufacture Ti + TiC MMCs with various pre-mixed ratios of TiC (10, 20 and 40 vol.%) The mechanical testing, including UTS, YS, elongation, hardness, and wear, were conducted. The results are presented in Figure 8. It can be observed that the UTS slightly deviates with the accumulation of TiC; meanwhile, YS declines quickly, which is caused by the existence of solid and stiff TiC particulates. The hardness and wear resistance of the produced MMCs raised with the increment in TiC volume fraction due to the strengthening effect of the particulates and the optimum bonding between TiC and Ti. Based on the excellent adhesion between TiC + Ti MMCs, such coatings can be deposited on the surfaces, where superior wear resistance is required. The LMD process inherits the high laser energy density; moreover, Ti showed an excellent affinity to the Oxygen + Nitrogen, which was absorbed quickly in the interstitials. The combination of the aforementioned facts leads to strength increment. Furthermore, a declination in the elasticity was observed in the MMCs.

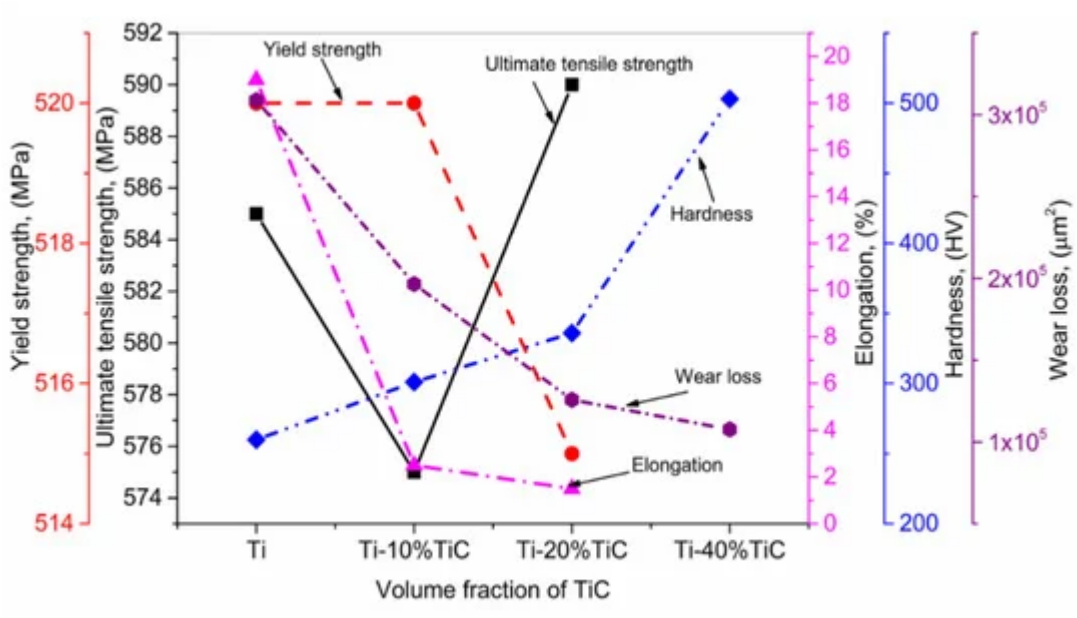

Figure 8. Effect of TiC reinforcement (vol.%) on ultimate tensile and yield strengths, elongation, hardness, and wear loss; based on the data provided in Ref. [82].

Table 5 provides a summary of the above-mentioned mechanical properties.

Table 5. Summary of MMCs mechanical properties.

Study by	MMCs by LMD	Hardness (HV)	Ultimate Tensile Strength (MPa)	Yield Strength (MPa)	Elongation (%)	Wear Loss (μm^2)	References
Li et al.	WC + Ti-wire	500	-	-	-	-	[83]
Bi et al.	Inconel 625 + TiC particulates (0.25/99.75;	285; 310; 312; 320	840; 930; 980; 990	530; 650;	16; 19; 28; 21	-	[77]

Study by	MMCs by LMD	Hardness (HV)	Ultimate Tensile Strength (MPa)	Yield Strength (MPa)	Elongation (%)	Wear Loss (μm^2)	References
	0.50/99.50; 1.0/99.0)			642; 690			
Gopagoni et al.	Nickel (80 wt.%) + Titanium (10 wt.%) + Carbon (10 wt.%)	370	-	-	-	-	[78]
Wang et al.	TiC particulates (0; 5; 10; 15; 20; 30 vol.%) + Ti6Al4V	375; 425; 427; 432; 475; 477	1100; 1200; 1100; 1000; 900; 700	-	5; 1; 0.8; 0.7; 0.5; 0.1	-	[79]
Hong et al.	Inconel 718 + TiC (Laser energy = 80; 100; 120; 160 kJ/m)	375; 400; 410; 450	-	-	-	-	[80]
Sateesh et al.	Ni-P + SiC (0; 1; 3; 5 wt.%)	300; 350; 390; 375	800; 900; 910; 300	400; 400; 410; 200	12; 14; 15; 2	-	[81]
Zhang et al.	Ti+TiC (10; 20; 40 vol.%)	260; 301; 336; 503	585; 575; 590; -	520; 520; 515; -	19; 2.5; 1.5; -	309,022.1; 196,579.5; 125,786.7; 107,735.6	[82]

Liu et al. [84] analyzed the creep performance of TA15-Ti + TiC particulates (10.8 vol.%) MMCs at 873 and 923 K, respectively, deposited by the LMD. The creep resistance of the MMCs improved notably due to the accumulation of TiC reinforcing particulates in comparison to the monolithic TA15-Ti alloy designed in between 723 to 773 K. The creep life for TA15-Ti + TiC MMCs at 873 and 923 K, is shown in Figure 9a. The rupture of the TiC + TA15 MMCs was originated due to the particles' cracking, interfacial debonding and voiding, which becomes dominant with the temperature elevation. Jiang and Kovacevic [85] performed a study on the behavior of TiC + H13 tool steel MMCs, manufactured by LMD. The influence of TiC (vol.%) on erosion resistance was analyzed. Figure 9b shows the erosion rates of the coated layers at different impact angles. For all the coatings, it can be observed that the impact angle influenced the erosion rate considerably. For the 30° impact angle, the lowest erosion rate was observed, followed by a 90° impact angle. The maximum erosion was found at 45° and 60° angles. Moreover, TiC with 80 (vol.%) presented the least erosion resistance, while the coating with 40 (vol.%) showed the highest ones.

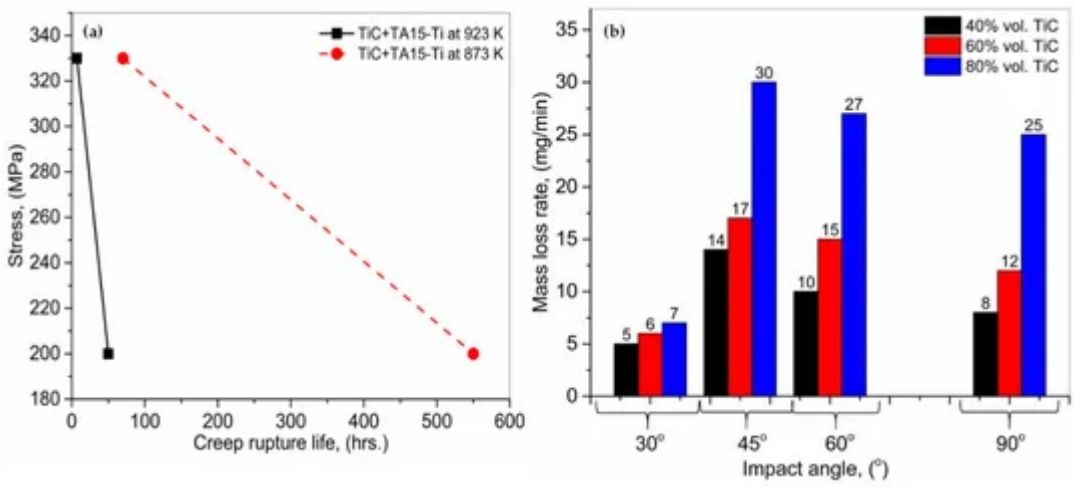

Figure 9. (**a**) Creep behavior of TiC + TA15-Ti MMCs, and (**b**) erosion rates for 40, 60, and 80 (vol.%) TiC + H13 tool steel MMCs at various impact angles; based on the data provided in Ref. [84][85].

Lei et al. [86] used the LMD for Si_p + 6063Al MMCs for 5, 12, 20 and 30 (wt.%) Si contents. The thermophysical properties of MMCs were investigated. The results are shown in Figure 10. They found that with the increment in Si (wt.%), the thermal conductivity of the MMCs declined due to the decrease in an α-Al phase, which exhibits the high-level conductivity. The thermal expansion coefficient presented an opposite behavior as compared to the thermal conductivity.

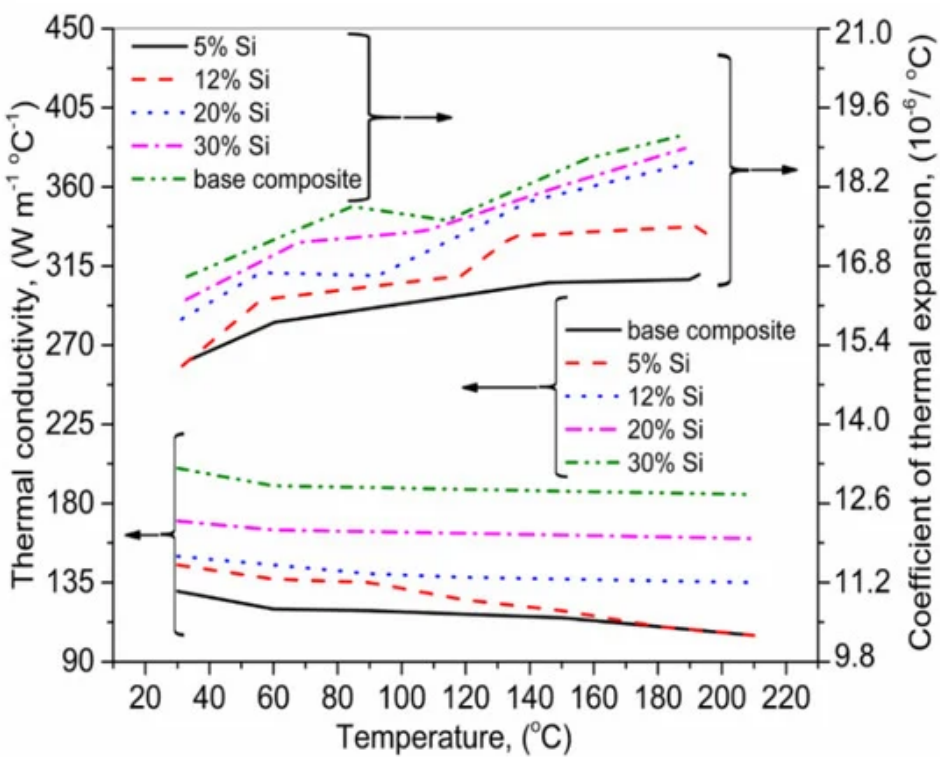

Figure 10. The relation between temperature and various fractions of Si on thermal conductivity and thermal expansion coefficient; based on the data provided in Ref. [86].

6. Applications of MMCs

The literature survey revealed the following main areas proposed by various studies.

6.1. Biomedical

MMCs have outstanding load-bearing and wear resistance properties, which make them interesting for implant applications [87]. TiN and SiC reinforced TMCs [88][89] have been proved for excellent biocompatibility. Hence, they are used for cladding on the metallic substrates to upgrade the biocompatibility of implants. In vitro testing was carried out to assess the biocompatibility of the deposited layers. The results showed an excellent cell to material interaction, and no toxicity was found. It showed that they could be used for load-bearing implants such as hip, knee and shoulder joints [88][89]. Moreover, orthopedic bone prototypes and meshed cranial prostheses implants were successfully developed for biomedical applications [90][91][92].

6.2. Wear Resistance

In MMCs, the ceramic reinforcements within the matrix play as the load-bearing element, which can confine the plastic distortion, thus, preventing the matrix from deterioration. It makes MMCs a potential candidate for wear-resistant applications [93][94]. The depositions of TiN reinforced MMCs on a Ni-Ti substrate by LMD, in a nitrogen atmosphere, increased the substrate' wear resistance by a factor of two [95]. TiB + TiN MMCs were prepared on a Ti-substrate using pre-mixed boron nitride (BN) + Ti6Al4V powders by the LMD. With the increase in the BN content up to 15 (wt.%), the surface hardness increased from 543 to 877 HV, thereby, increasing the wear resistivity of the deposited layers [96]. The deposition of WC/W_2C + Ni MMCs on steel substrate was carried out via LMD. It was found that an inclination in the WC/W_2C content and a declination in carbide dimension, can enhance the wear resistance of MMCs up to 200 times more than the pure Ni matrix [97]. The dry friction, along with better contact load, is an increasing demand for aerospace and heavy industries. In simple words, only the high wear resistance is not sufficient. For this difficulty, WC/Co (ceramic reinforcement) + Cu-Sn (solid lubricant) were manufactured by the LMD process. The developed structures presented better wear resistance and low frictional characteristics [98].

6.3. Corrosion and Erosion Resistance

MMCs are used to increase electrochemical corrosion and erosion resistance. For this purpose, Ni_2Si composites were deposited on a steel substrate by the LMD technique [99]. Immersion and anodic polarization tests were conducted, which proved the deposited layer intermediated better bio- and electrochemical corrosion resistance. The novel layers of TiC + Satellite 6, WC + Co, $MoSi_2$ + stellate 6, and $MoSi_2$ + steel matrix composites, were deposited on a metallic substrate to improve erosion wear rate [100].

6.4. Industrial

LMD technology has recently been used to repair brake disks and turbo-engine parts [101]. In one of the recent studies, LMD was demonstrated as a potential candidate to repair steel dies using the Fe-Cr and Fe-Ni layers [102]. Moreover, various applications of the LMD have been determined in the fields of aeronautics and refractory [103]. Furthermore, LMD technique has been tested for the manufacturing of multiple parts, including turbine and compressor blades [104], nozzle guide vanes [105], jet engines [106], casting dies [107], Z-notches [108], bearing seats, valves, shafts, cylinders and rods [109], and seals [110].

7. MMCs by the LMD: Strengths, Challenges and Their Potential Solutions

On the one hand, MMCs produced by LMD show excellent hardness, toughness and frictional properties. On the other hand, MMCs loose ductility, YS, and UTS with the addition of ceramic particulates. Mechanical properties of MMCs primarily depend on the adhesion between ceramic reinforcements and metal matrices along with the interface. Zheng et al. [111][112] used an effective strategy to overcome such difficulties, by encapsulating ceramic particles within metallic coatings to strengthen the inconel-625 + Ti-6Al-4V MMCs. This method prevents the bunching of ceramic particles within MMCs, thus, effectively reducing the voids and cracks formation in between metal and ceramic intersection. There are various hindrances for obtaining the fully dense and homogenized MMCs. The dense MMCs are restricted due to micro/macro-cracks, gas entrapment, and particulate accumulation during the printing process.

Moreover, if the initially deposited layers are poorly bonded to the substrate, the following layers deposition will result in an up-warp, hence, resulting in manufacturing failure [113]. Due to rapid heating and solidification in the LMD process, cracks are usually induced due to the large thermal gradient [114]. These cracks decrease the lifetime of the fabricated parts. The cracks can cause the catastrophic failure of the deposited layers under cyclic loading [115]. Therefore, it is extremely important to manufacture fully dense parts [116][117][118]. Various methods can solve the problems as mentioned above: (a) Process optimization [119][120], (b) integrating the LMD process with assisting technology such as ultrasonic vibration [121][122], (c) pre/post-heating the substrate to decrease thermal gradient [123][124], (d) adding rare earth oxides to change the melt pool dynamics [125][126] and (e) tailoring the novel structures [127][128].

8. Future Research Directions in MMCs

Based on the current review, a few potential areas still need attention from the researchers. In the LMD process, strong bonding between the deposited MMCs layers with the substrate is of great importance to fabricate bulk parts. One of the ways to achieve the desired strength is “process optimization.” However, in situations where process optimization fails, integrating an assisting technology such as ultrasonic vibration with LMD can be a decent alternative to secure an optimum bonding between the deposited layers and substrate.

Moreover, the post-processing needs special tools and high energy, thus, increasing the fabrication cost. This high cost limits the availability of MMCs to niche applications. There is a need to find out a balanced solution between better thermo-mechanical properties and low production cost, which can promote the MMCs effectively.

Depending on the amount of the dispersed phase within the composition, MMCs can display new properties or an enhancement of the existing ones. By simultaneous addition of matrix and reinforcement in powder form, might result in new materials with exciting properties. In addition, parts with complex architecture such as multilayered structures or gradient composition can be easily obtained via in-situ MMCs. Another area to explore is to manufacture the exact composition of MMCs via different laser sources as it may affect microstructure, mechanical, thermal and electrical properties significantly.

LMD is not suitable for the parts with fine geometry in the range of hundred-microns. On the other hand, SLM is a technique appropriate for metal parts with lattice structures and complex geometries. However, LMD scanning heads future developments can allow the obtaining of sub-mm resolutions. Hence, an increase in resolution for the MMCs printing via the LMD is a new area to be explored.

The newest trend in 3D printing is the use of enhanced topology. The CAD/CAM user specifies the part size, restrictions and the acting forces into the dedicated software. With this data, the software calculates and proposes the best shape regarding user’s requirements and the maximum resistance to the forces that will act upon it. However, the shape offered by the software is most of the time, unconventional and convoluted. Conventional casting or pressing techniques are often inappropriate for producing it, while 3D printing, in this case, is a suitable choice for building such parts. LMD printing method can advance this field even more by involving MMCs.

References

1. Yingbin Hu; Weilong Cong; A review on laser deposition-additive manufacturing of ceramics and ceramic reinforced metal matrix composites. *Ceramics International* **2018**, *44*, 20599-20612, 10.1016/j.ceramint.2018.08.083.
2. Bernhard Mueller; Detlef Kochan; Laminated object manufacturing for rapid tooling and patternmaking in foundry industry. *Computers in Industry* **1999**, *39*, 47-53, 10.1016/s0166-3615(98)00127-4.
3. Dr. Kumar Sundaram—Ex-situ and in-situ Metal Matrix Composites. Available online: https://sites.google.com/site/kumarspage/Home/research/ex-situ-and-in-situ-composites (accessed on 21 October 2019).
4. Zhou, W.; Xu, Z.M. Casting of SiC reinforced metal matrix composites. J. Mater. Process. Technol. 1997, 63, 358–363. [Google Scholar] [CrossRef]
5. Gupta, M.; Lai, M.O.; Lim, C.Y.H. Development of a novel hybrid aluminum-based composite with enhanced properties. J. Mater. Process. Technol. 2006, 176, 191–199. [Google Scholar]

[CrossRef]

6. Ourdjini, A.; Chew, K.C.; Khoo, B.T. Settling of silicon carbide particles in cast metal matrix composites. J. Mater. Process. Technol. 2001, 116, 72–76. [Google Scholar] [CrossRef]
7. Srivatsan, T.S.; Sudarshan, T.S.; Lavernia, E.J. Processing of discontinuously-reinforced metal matrix composites by rapid solidification. Prog. Mater. Sci. 1995, 39, 317–409. [Google Scholar] [CrossRef]
8. Manna, A.; Mahapatra, P.B.; Bains, H.S. Experimental study on fabrication of Al-Al2O3/Grp metal matrix composites. J. Compos. Mater. 2010, 44, 3069–3079.
9. Naher, S.; Brabazon, D.; Looney, L. Development and assessment of a new quick quench stir caster design for the production of metal matrix composites. J. Mater. Process. Technol. 2005, 166, 430–439. [Google Scholar] [CrossRef]
10. Flemings, M.C. Behavior of metal alloys in the semisolid state. Metall. Trans. A 1991, 22, 957–981.
11. Narasimha, B.G.; Krishna, V.M.; Xavior, A.M. A review on processing of particulate metal matrix composites and its properties. Int. J. Appl. Eng. Res. 2013, 8, 647–666. [Google Scholar]
12. Williams, G.; Fisher, K.M. Squeeze forming of aluminium-alloy components. Met. Technol. 1981, 8, 263–267. [Google Scholar] [CrossRef]
13. Ghomashchi, M.R.; Vikhrov, A. Squeeze casting: An overview. J. Mater. Process. Technol. 2000, 101, 1–9. [Google Scholar] [CrossRef]
14. Schwam, D.; Wallace, J.F.; Chang, Q.; Zhu, Y.; Schwam, D.; Wallace, J.F.; Chang, Q.; Zhu, Y. Optimization of the squeeze casting process for aluminum alloy parts. STIN 2002, 3, 01652.
15. Das, S.; Behera, R.; Datta, A.; Majumdar, G.; Oraon, B.; Sutradhar, G. Experimental investigation on the effect of reinforcement particles on the forgeability and the mechanical properties of aluminum metal matrix composites. Mater. Sci. Appl. 2010, 1, 310–316. [Google Scholar] [CrossRef]
16. Manjunathal, H.; Dinesh, P. Fabrication and properties of dispersed carbon nanotube-Al6061 composites. Int. J. Innov. Res. Sci. Eng. Technol. 2013, 2, 500–507.
17. Barekar, N.S.; Patel, J.B.; Barekar, N.; Tzamtzis, S.; Dhindaw, B.K.; Patel, J.; Babu, N.H.; Fan, Z. Processing of aluminum-graphite particulate metal matrix composites by advanced shear technology. J. Mater. Eng. Perform. 2009, 18, 1230–1240. [Google Scholar] [CrossRef]
18. Barekar, N.S.; Tzamtzis, S.; Hari Babu, N.; Fan, Z.; Dhindaw, B.K. Processing of ultrafine-size particulate metal matrix composites by advanced shear technology. Metall. Mater. Trans. A Phys. Metall. Mater. Sci. 2009, 40, 691–701.

19. Suneel Donthamsetty; Nageswara Rao. D; Investigation on mechanical properties of a356 nanocomposites fabricated by ultrasonic assisted cavitation. *Journal of Mechanical Engineering* **2011**, *41*, 121-129, 10.3329/jme.v41i2.7507.
20. Sato, Y.S.; Nelson, T.W.; Sterling, C.J. Recrystallization in type 304L stainless steel during friction stirring. Acta Mater. 2005, 53, 637–645. [Google Scholar] [CrossRef]
21. Chen, C.L.; Tatlock, G.J.; Jones, A.R. Microstructural evolution in friction stir welding of nanostructured ODS alloys. J. Alloys Compd. 2010, 504, S460–S466.
22. Briac Lanfant; Florian Bär; Antaryami Mohanta; Marc Leparoux; Fabrication of Metal Matrix Composite by Laser Metal Deposition-A New Process Approach by Direct Dry Injection of Nanopowders.. *Materials* **2019**, *12*, 3584, 10.3390/ma12213584.
23. D. Liu; S.Q. Zhang; A. Li; H.M. Wang; High temperature mechanical properties of a laser melting deposited TiC/TA15 titanium matrix composite. *Journal of Alloys and Compounds* **2010**, *496*, 189-195, 10.1016/j.jallcom.2010.02.120.
24. D. Liu; S.Q. Zhang; A. Li; H.M. Wang; Microstructure and tensile properties of laser melting deposited TiC/TA15 titanium matrix composites. *Journal of Alloys and Compounds* **2009**, *485*, 156-162, 10.1016/j.jallcom.2009.05.112.
25. D.E. Cooper; N. Blundell; S. Maggs; G.J. Gibbons; Additive layer manufacture of Inconel 625 metal matrix composites, reinforcement material evaluation. *Journal of Materials Processing Technology* **2013**, *213*, 2191-2200, 10.1016/j.jmatprotec.2013.06.021.
26. Fritz Klocke; Kristian Arntz; Mahesh Teli; Kai Winands; Maximilian Wegener; Stella Oliari; State-of-the-art Laser Additive Manufacturing for Hot-work Tool Steels. *Procedia CIRP* **2017**, *63*, 58-63, 10.1016/j.procir.2017.03.073.
27. Li, F.; Gao, Z.; Zhang, Y.; Chen, Y. Alloying effect of titanium on WCp/Al composite fabricated by coincident wire-powder laser deposition. Mater. Des. 2016, 93, 370–378. [Google Scholar] [CrossRef]
28. Kaierle, S.; Barroi, A.; Noelke, C.; Hermsdorf, J.; Overmeyer, L.; Haferkamp, H. Review on laser deposition welding: From micro to macro. Phys. Procedia 2012, 39, 336–345. [Google Scholar] [CrossRef]
29. Shishkovsky, I.; Missemer, F.; Smurov, I. Direct metal deposition of functional graded structures in Ti-Al System. Phys. Procedia 2012, 39, 382–391. [Google Scholar] [CrossRef]
30. Oliari, S.H.; D'Oliveira, A.S.C.M.; Schulz, M.; Oliari, S.H.; D'Oliveira, A.S.C.M.; Schulz, M. Additive manufacturing of H11 with wire-based laser metal deposition. Soldag. Inspeção 2017, 22, 466–479. [Google Scholar] [CrossRef]

31. Keicher, D.M.; Smugeresky, J.E. The laser forming of metallic components using particulate materials. JOM. 1997, 49, 51–54.
32. Peter Kayode Farayibi; J. A. Folkes; Adam T. Clare; Laser Deposition of Ti-6Al-4V Wire with WC Powder for Functionally Graded Components. *Materials and Manufacturing Processes* **2013**, *28*, 514-518, 10.1080/10426914.2012.718477.
33. P.K. Farayibi; T. E. Abioye; A.R. Kennedy; A.T. Clare; Development of metal matrix composites by direct energy deposition of ‘satellited’ powders. *Journal of Manufacturing Processes* **2019**, *45*, 429-437, 10.1016/j.jmapro.2019.07.029.
34. A. Ramakrishnan; Guru Prasad Dinda; Microstructural control of an Al–W aluminum matrix composite during direct laser metal deposition. *Journal of Alloys and Compounds* **2020**, *813*, 152208, 10.1016/j.jallcom.2019.152208.
35. Zhenglong Lei; Jiang Bi; Yanbin Chen; Xi Chen; Ze Tian; Xikun Qin; Effect of TiB2 content on microstructural features and hardness of TiB2/AA7075 composites manufactured by LMD. *Journal of Manufacturing Processes* **2020**, *53*, 283-292, 10.1016/j.jmapro.2020.02.036.
36. X. Li; C.H. Zhang; S. Zhang; C.L. Wu; J.B. Zhang; H.T. Chen; Adil O Abdullah; Design, preparation, microstructure and properties of novel wear-resistant stainless steel-base composites using laser melting deposition. *Vacuum* **2019**, *165*, 139-147, 10.1016/j.vacuum.2019.04.016.
37. Peters, M.; Kumpfert, J.; Ward, C.H.; Leyens, C. Titanium alloys for aerospace applications. Adv. Eng. Mater. 2003, 5, 419–427. [Google Scholar] [CrossRef]
38. Ravi Chandran, K.S.; Panda, K.B.; Sahay, S.S. TiBw-reinforced Ti composites: Processing, properties, application prospects, and research needs. JOM. 2004, 56, 42–48. [Google Scholar] [CrossRef]
39. Hayat, M.D.; Singh, H.; He, Z.; Cao, P. Titanium metal matrix composites: An overview. Compos. Part A Appl. Sci. Manuf. 2019, 121, 418–438.
40. Margherita Stefania Sciolti; Mariaenrica Frigione; Maria Antonietta Aiello; Wet Lay-Up Manufactured FRPs for Concrete and Masonry Repair: Influence of Water on the Properties of Composites and on Their Epoxy Components. *Journal of Composites for Construction* **2010**, *14*, 823-833, 10.1061/(asce)cc.1943-5614.0000132.
41. D. R. Pank; J. J. Jackson; Metal- matrix composite processing technologies for aircraft engine applications. *Journal of Materials Engineering and Performance* **1993**, *2*, 341-346, 10.1007/bf02648820.
42. Chris Lobley; Zhengxiao Guo; Viable Routes to Large-scale Commercialisation of Silicon Carbide Fibre Titanium Matrix Composites. *Materials Technology* **1999**, *14*, 133-138, 10.1080/10667857.1999.11752829.

43. C. M. Lobley; Z. X. Guo; Processing of Ti-SiC metal matrix composites by tape casting. *Materials Science and Technology* **1998**, *14*, 1024-1028, 10.1179/mst.1998.14.9-10.1024.
44. Kondoh, K. Titanium Powder Metallurgy: Science, Technology and Applications; Elsevier Inc.: Amsterdam, The Netherlands, 2015; pp. 277–297. ISBN 9780128009109. [Google Scholar]
45. Huang, L.; Geng, L. Discontinuously reinforced titanium matrix composites; Springer: Berlin, Germany, 2017; ISBN 978-981-10-4449-6.
46. Vert, R.; Pontone, R.; Dolbec, R.; Dionne, L.; Boulos, M.I. Induction plasma technology applied to powder manufacturing: Example of titanium-based materials. Key Eng. Mater. 2016, 704, 282–286. [Google Scholar] [CrossRef]
47. Fan, Z.; Miodownik, A.P.; Chandrasekaran, L.; Ward-Close, M. The Young's moduli of in situ Ti/TiB composites obtained by rapid solidification processing. J. Mater. Sci. 1994, 29, 1127–1134. [Google Scholar] [CrossRef]
48. Gofrey, T.M.T.; Goodwin, P.S.; Ward-Close, C.M. Titanium particulate metal matrix composites - reinforcement, production methods, and mechanical properties. Adv. Eng. Mater. 2000, 2, 85–91.
49. Tushar Borkar; Sundeep Gopagoni; Soumya Nag; J. Y. Hwang; Peter Collins; Rajarshi Banerjee; In situ nitridation of titanium–molybdenum alloys during laser deposition. *Journal of Materials Science* **2012**, *47*, 7157-7166, 10.1007/s10853-012-6656-z.
50. G. Sivakumar; V. Ananthi; S. Ramanathan; Production and mechanical properties of nano SiC particle reinforced Ti–6Al–4V matrix composite. *Transactions of Nonferrous Metals Society of China* **2017**, *27*, 82-90, 10.1016/s1003-6326(17)60009-8.
51. Morsi, K.; Patel, V.V. Processing and properties of titanium-titanium boride (TiBw) matrix composites—A review. J. Mater. Sci. 2007, 42, 2037–2047. [Google Scholar] [CrossRef]
52. Geng, L.; Ni, D.R.; Zhang, J.; Zheng, Z.Z. Hybrid effect of TiBw and TiCp on tensile properties of in situ titanium matrix composites. J. Alloys Compd. 2008, 463, 488–492.
53. N. Shivakumar; V. Vasu; N. Narasaiah; Subodh Kumar; Synthesis and Characterization of Nano-sized Al2O3 Particle Reinforced ZA-27 Metal Matrix Composites. *Procedia Materials Science* **2015**, *10*, 159-167, 10.1016/j.mspro.2015.06.037.
54. Dougherty, T.; Xu, Y.; Hanizan, A. Mechanical properties and microstructure of PM Ti-Si3N4 discontinuous fibre composite. In Proceedings of the TMS Annual Meeting; Wiley: Hoboken, NJ, USA, 2016; pp. 721–728. [Google Scholar]
55. Saito, T. The automotive application of discontinuously reinforced TiB-Ti composites. JOM 2004, 56, 33–36. [Google Scholar] [CrossRef]
56. Munir, K.S.; Kingshott, P.; Wen, C. Carbon nanotube reinforced titanium metal matrix composites prepared by powder metallurgy - A review. Crit. Rev. Solid State Mater. Sci. 2015, 40, 38–55.

[Google Scholar] [CrossRef]

57. Metcalfe, A.G. Interaction and fracture of titanium-boron composites. J. Compos. Mater. 1967, 1, 356–365. [Google Scholar] [CrossRef]
58. Smith, P.R.; Froes, F.H. Developments in titanium metal matrix composites. JOM J. Miner. Met. Mater. Soc. 1984, 36, 19–26. [Google Scholar] [CrossRef]
59. NASA Technical Reports Server (NTRS) - Control of interface reactions in SIC/TI composites. Available online: https://ntrs.nasa.gov/search.jsp?R=19820009392 (accessed on 3 November 2019).
60. Guo, S. Fiber size effects on mechanical behaviours of SiC fibres-reinforced Ti3AlC2 matrix composites. J. Eur. Ceram. Soc. 2017, 37, 5099–5104. [Google Scholar] [CrossRef]
61. Thurston, J.R. Elevated temperature tensile and creep behavior of a SiC fiber-reinforced titanium metal matrix composite; Final Report; Ohio Aerospace Institute: Cleveland, OH, USA, 4 January 1995. [Google Scholar]
62. MacKay, R.A.; Brindley, P.K.; Froes, F.H. Continuous fiber-reinforced titanium aluminide composites. JOM 1991, 43, 23–29. [Google Scholar] [CrossRef]
63. Pellous, R.M. Composites Research in Support of the Nasp Institute for Composites (NIC); Final Report; Massachusetts Institute of Technology: Cambridge, MA, USA, 1994. [Google Scholar]
64. Kingston, W.R. Carbon-Titanium Composites. U.S. Patent 5,733,390, 31 March 1998. [Google Scholar]
65. Wu, T.; Qiao, J.; Jiang, D. Preparation and properties of carbon fiber/titanium alloy composite for automobile. In Proceedings of SAE-China Congress 2015: Selected Papers; Springer: Singapore, 2016; Volume 364, pp. 289–295. [Google Scholar]
66. Smith, P.R.; Gambone, M.L.; Williams, D.S.; Garner, D.I. Heat treatment effects on SiC fiber. J. Mater. Sci. 1998, 33, 5855–5872. [Google Scholar] [CrossRef]
67. Baker, A.M.; Grant, P.S.; Jenkins, M.L. The response of SiC fibres to vacuum plasma spraying and vacuum hot pressing during the fabrication of titanium matrix composites. J. Microsc. 1999, 196, 162–174. [Google Scholar] [CrossRef]
68. Chen Hong; Dongdong Gu; Donghua Dai; Moritz AlKhayat; Wolf Urban; Pengpeng Yuan; Sainan Cao; Andres Gasser; Andreas Weisheit; Ingomar Kelbassa; et al.Minlin ZhongReinhart Poprawe Laser additive manufacturing of ultrafine TiC particle reinforced Inconel 625 based composite parts: Tailored microstructures and enhanced performance. *Materials Science and Engineering: A* **2015**, *635*, 118-128, 10.1016/j.msea.2015.03.043.
69. Yuxin Li; Peikang Bai; Yaomin Wang; Jiandong Hu; Zuoxing Guo; Effect of TiC content on Ni/TiC composites by direct laser fabrication. *Materials & Design* **2009**, *30*, 1409-1412, 10.1016/j.matde

s.2008.06.046.

70. Xiao Chun Li; Jürgen Stampfl; Fritz B Prinz; Mechanical and thermal expansion behavior of laser deposited metal matrix composites of Invar and TiC. *Materials Science and Engineering: A* **2000**, *282*, 86-90, 10.1016/s0921-5093(99)00781-9.
71. Xiong, Y.; Smugeresky, J.E.; Schoenung, J.M. The influence of working distance on laser deposited WC-Co. J. Mater. Process. Technol. 2009, 209, 4935–4941. [Google Scholar] [CrossRef]
72. Xiong, Y.; Smugeresky, J.E.; Ajdelsztajn, L.; Schoenung, J.M. Fabrication of WC-Co cermets by laser engineered net shaping. Mater. Sci. Eng. A 2008, 493, 261–266. [Google Scholar] [CrossRef]
73. Picas, J.A.; Xiong, Y.; Punset, M.; Ajdelsztajn, L.; Forn, A.; Schoenung, J.M. Microstructure and wear resistance of WC-Co by three consolidation processing techniques. Int. J. Refract. Met. Hard Mater. 2009, 27, 344–349. [Google Scholar] [CrossRef]
74. J. Choi; J. Mazumder; Non-equilibrium synthesis of Fe-Cr-C-W alloy by laser cladding. *Journal of Materials Science* **1994**, *29*, 4460-4476, 10.1007/bf00376268.
75. Xiangyang Xu; Minlin Zhong; Wenjin Liu; Hongqing Sun; Laser synthesizing particulate reinforced NiAl intermetallic matrix composite. *International Congress on Applications of Lasers & Electro-Optics* **2004**, *16*, 160, 10.2351/1.5065600.
76. Composite Materials Processing and applications of MMCs. Available online: http://metalurji.mu.edu.tr/Icerik/metalurji.mu.edu.tr/Sayfa/CompositeMaterials6(1).pdf (accessed on 26 February 2020).
77. Bi, G.; Sun, C.N.; Nai, M.L.; Wei, J. Micro-structure and mechanical properties of nano-TiC reinforced Inconel 625 deposited using LAAM. In Proceedings of the Physics. Procedia; Elsevier B.V.: Amsterdam, The Netherlands, 2013; Volume 41, pp. 828–834.
78. Gopagoni, S.; Hwang, J.Y.; Singh, A.R.P.; Mensah, B.A.; Bunce, N.; Tiley, J.; Scharf, T.W.; Banerjee, R. Microstructural evolution in laser deposited nickel-titanium-carbon in situ metal matrix composites. J. Alloys Compd. 2011, 509, 1255–1260.
79. Wang, J.; Li, L.; Tan, C.; Liu, H.; Lin, P. Microstructure and tensile properties of TiCp/Ti6Al4V titanium matrix composites manufactured by laser melting deposition. J. Mater. Process. Technol. 2018, 252, 524–536.
80. Hong, C.; Gu, D.; Dai, D.; Gasser, A.; Weisheit, A.; Kelbassa, I.; Zhong, M.; Poprawe, R. Laser metal deposition of TiC/Inconel 718 composites with tailored interfacial microstructures. Opt. Laser Technol. 2013, 54, 98–109.

81. Sateesh, N.H.; Mohan Kumar, G.C.; Krishna, P. Influence of Ni-P coated SiC and laser scan speed on the microstructure and mechanical properties of IN625 metal matrix composites. Lasers Manuf. Mater. Process. 2015, 2, 187–198.
82. Zhang, Y.; Wei, Z.; Shi, L.; Xi, M. Characterization of laser powder deposited Ti-TiC composites and functional gradient materials. J. Mater. Process. Technol. 2008, 206, 438–444.
83. Li, F.; Gao, Z.; Li, L.; Chen, Y. Microstructural study of MMC layers produced by combining wire and coaxial WC powder feeding in laser direct metal deposition. Opt. Laser Technol. 2016, 77, 134–143.
84. Liu, D.; Zhang, S.Q.; Li, A.; Wang, H.M. Creep rupture behaviors of a laser melting deposited TiC/TA15 in situ titanium matrix composite. Mater. Des. 2010, 31, 3127–3133.
85. Jiang, W.H.; Kovacevic, R. Laser deposited TiC/H13 tool steel composite coatings and their erosion resistance. J. Mater. Process. Technol. 2007, 186, 331–338.
86. Lei, Z.; Tian, Z.; Li, P.; Chen, Y.; Zhang, H.; Gu, J.; Su, X. Effect of Si content on microstructure and thermo-physical properties of the joint of Sip/6063Al composite by laser melting deposition. Opt. Laser Technol. 2017, 97, 116–123.
87. Das, M.; Balla, V.K.; Kumar, T.S.S.; Manna, I. Fabrication of biomedical implants using laser engineered net shaping (LENSTM). Trans. Indian Ceram. Soc. 2013, 72, 169–174.
88. Balla, V.K.; Bhat, A.; Bose, S.; Bandyopadhyay, A. Laser processed TiN reinforced Ti6Al4V composite coatings. J. Mech. Behav. Biomed. Mater. 2012, 6, 9–20.
89. Das, M.; Balla, V.K.; Kumar, T.S.S.; Bandyopadhyay, A.; Manna, I. Tribological, electrochemical and in vitro biocompatibility properties of SiC reinforced composite coatings. Mater. Des. 2016, 95, 510–517.
90. Chioibasu, D.; Achim, A.; Popescu, C.; Stan, G.; Pasuk, I.; Enculescu, M.; Iosub, S.; Duta, L.; Popescu, A. Prototype orthopedic bone plates 3D printed by laser melting deposition. Materials 2019, 12, 906.
91. Florian, P.E.; Duta, L.; Grumezescu, V.; Popescu-Pelin, G.; Popescu, A.C.; Oktar, F.N.; Evans, R.W.; Roseanu Constantinescu, A. Lithium-doped biological-derived hydroxyapatite coatings sustain in vitro differentiation of human primary mesenchymal stem cells to osteoblasts. Coatings 2019, 9, 781.
92. Chioibasu, D.; Duta, L.; Popescu-Pelin, G.; Popa, N.; Milodin, N.; Iosub, S.; Balescu, L.M.; Catalin Galca, A.; Claudiu Popa, A.; Oktar, F.N.; et al. Animal origin bioactive hydroxyapatite thin films synthesized by RF-magnetron sputtering on 3D printed cranial implants. Metals 2019, 9, 1332.
93. Hu, Y.; Ning, F.; Wang, H.; Cong, W.; Zhao, B. Laser engineered net shaping of quasi-continuous network microstructural TiB reinforced titanium matrix bulk composites: Microstructure and wear

performance. Opt. Laser Technol. 2018, 99, 174–183.

94. Weng, F.; Chen, C.; Yu, H. Research status of laser cladding on titanium and its alloys: A review. Mater. Des. 2014, 58, 412–425.
95. Man, H.C.; Zhang, S.; Cheng, F.T.; Guo, X. In situ formation of a TiN/Ti metal matrix composite gradient coating on NiTi by laser cladding and nitriding. Surf. Coatings Technol. 2006, 200, 4961–4966.
96. Das, M.; Balla, V.K.; Basu, D.; Manna, I.; Sampath Kumar, T.S.; Bandyopadhyay, A. Laser processing of in situ synthesized TiB-TiN-reinforced Ti6Al4V alloy coatings. Scr. Mater. 2012, 66, 578–581.
97. Van Acker, K.; Vanhoyweghen, D.; Persoons, R.; Vangrunderbeek, J. Influence of tungsten carbide particle size and distribution on the wear resistance of laser clad WC/Ni coatings. In Proceedings of the Wear; Elsevier: Amsterdam, The Netherlands, 2005; Volume 258, pp. 194–202.
98. Smurov, I. Laser cladding and laser assisted direct manufacturing. Surf. Coatings Technol. 2008, 202, 4496–4502.
99. Wang, H.M.; Wang, C.M.; Cai, L.X. Wear and corrosion resistance of laser clad Ni2Si/NiSi composite coatings. Surf. Coatings Technol. 2003, 168, 202–208.
100. Tucker, T.R.; Clauer, A.H.; Wright, I.G.; Stropki, J.T. Laser-processed composite metal cladding for slurry erosion resistance. Thin Solid Films 1984, 118, 73–84
101. Gasser, A.; Backes, G.; Kelbassa, I.; Weisheit, A.; Wissenbach, K. Laser additive manufacturing. Laser Tech. J. 2010, 7, 58–63.
102. Jang, J.H.; Mun, S.M.; Sung, M.Y.; Moon, Y.H. Application of direct laser melting to restore damaged steel dies. Met. Mater. Int. 2011, 17, 167–174.
103. Wang, H.M.; Zhang, L.Y.; Li, A.; Tang, H.B.; Zhang, S.Q.; Fang, Y.L.; Li, P. Progress on laser melting deposition processing and manufacturing of advanced aeronautical metallic structural materials and coatings. Heat Treat. Met. 2008, 33, 82–85.
104. Qi, H.; Azer, M.; Singh, P. Adaptive toolpath deposition method for laser net shape manufacturing and repair of turbine compressor airfoils. Int. J. Adv. Manuf. Technol. 2010, 48, 121–131.
105. Kelbassa, I.; Albus, P.; Dietrich, J.; Wilkes, J. Manufacture and Repair of Aero Engine Components Using Laser Technology. In Proceedings of the 3rd Pacific International Conference on Application of Lasers and Optics, Beijing, China, 16–18 April 2008.
106. Pratt, V.D.; Scheidt, W.D.; Whitney, E.J. Fabrication of Components by Layered Deposition. U.S. Patent 5,038,014, 6 August 1991.

107. Mazumder, J. Fabrication of Customized Die Inserts Using Closed-Loop Direct Metal Deposition (DMD). U.S. Patent 10/629,062, 5 February 2004.
108. Guo, W. Laser Powder Fusion Repair of Z-Notches with Nickel Based Superalloy Powder. U.S. Patent 7,009,137, 7 March 2006.
109. Kawasaki, M.; Takase, K.; Kato, S.; Nakagawa, M.; Mori, K.; Nemoto, M.; Takagi, S.; Sugimoto, H. Development of engine valve seats directly deposited onto aluminum cylinder head by laser cladding process. J. Engines 1992, 101, 1000–1014.
110. Withey, P.; Schlienger, M. Forming Structures by Laser Deposition. U.S. Patent 11/224,138, 16 March 2006.
111. Zheng, B.; Smugeresky, J.E.; Zhou, Y.; Baker, D.; Lavernia, E.J. Microstructure and properties of laser-deposited Ti6Al4V metal matrix composites using Ni-Coated powder. Metall. Mater. Trans. A Phys. Metall. Mater. Sci. 2008, 39 A, 1196–1205.
112. Zheng, B.; Topping, T.; Smugeresky, J.E.; Zhou, Y.; Biswas, A.; Baker, D.; Lavernia, E.J. The influence of Ni-coated TiC on laser-deposited IN625 metal matrix composites. Metall. Mater. Trans. A Phys. Metall. Mater. Sci. 2010, 41, 568–573.
113. Sayyad Amin, J.; Nikooee, E.; Ayatollahi, S.; Alamdari, A. Investigating wettability alteration due to asphaltene precipitation: Imprints in surface multifractal characteristics. Appl. Surf. Sci. 2010, 256, 6466–6472.
114. Hu, Y.; Ning, F.; Cong, W.; Li, Y.; Wang, X.; Wang, H. Ultrasonic vibration-assisted laser engineering net shaping of ZrO2-Al2O3 bulk parts: Effects on crack suppression, microstructure, and mechanical properties. Ceram. Int. 2018, 44, 2752–2760.
115. Ravi Chandran, K.S.; Panda, K.B.; Sahay, S.S. TiBw-reinforced Ti composites: Processing, properties, application prospects, and research needs. JOM. 2004, 56, 42–48.
116. Hu, Y.; Cong, W.; Wang, X.; Li, Y.; Ning, F.; Wang, H. Laser deposition-additive manufacturing of TiB-Ti composites with novel three-dimensional quasi-continuous network microstructure: Effects on strengthening and toughening. Compos. Part B Eng. 2018, 133, 91–100.
117. Attar, H.; Bönisch, M.; Calin, M.; Zhang, L.C.; Scudino, S.; Eckert, J. Selective laser melting of in situ titanium-titanium boride composites: Processing, microstructure and mechanical properties. Acta Mater. 2014, 76, 13–22.
118. Hu, Y.; Zhao, B.; Ning, F.; Wang, H.; Cong, W. In-situ ultrafine three-dimensional quasi-continuous network microstructural TiB reinforced titanium matrix composites fabrication using laser engineered net shaping. Mater. Lett. 2017, 195, 116–119.
119. Wu, Q.; Li, W.; Zhong, N.; Gang, W.; Haishan, W. Microstructure and wear behavior of laser cladding VC-Cr7C3 ceramic coating on steel substrate. Mater. Des. 2013, 49, 10–18.

120. Triantafyllidis, D.; Li, L.; Stott, F.H. Crack-free densification of ceramics by laser surface treatment. Surf. Coatings Technol. 2006, 201, 3163–3173.
121. Yang, Y.; Lan, J.; Li, X. Study on bulk aluminum matrix nano-composite fabricated by ultrasonic dispersion of nano-sized SiC particles in molten aluminum alloy. Mater. Sci. Eng. A 2004, 380, 378–383.
122. Ning, F.; Hu, Y.; Liu, Z.; Wang, X.; Li, Y.; Cong, W. Ultrasonic vibration-assisted laser engineered net shaping of inconel 718 parts: Microstructural and mechanical characterization. J. Manuf. Sci. Eng. Trans. ASME 2018, 140, 061012–061023.
123. Zhou, S.; Huang, Y.; Zeng, X.; Hu, Q. Microstructure characteristics of Ni-based WC composite coatings by laser induction hybrid rapid cladding. Mater. Sci. Eng. A 2008, 480, 564–572.
124. Liu, W.; DuPont, J.N. Fabrication of carbide-particle-reinforced titanium aluminide-matrix composites by laser-engineered net shaping. Metall. Mater. Trans. A Phys. Metall. Mater. Sci. 2004, 35, 1133–1140.
125. Wu, C.; Ma, M.; Liu, W.; Zhong, M.; Zhang, H.; Zhang, W. Laser cladding in-situ carbide particle reinforced Fe-based composite coatings with rare earth oxide addition. J. Rare Earths 2009, 27, 997–1002.
126. Niu, F.; Wu, D.; Ma, G.; Zhou, S.; Zhang, B. Effect of second-phase doping on laser deposited Al2O3 ceramics. Rapid Prototyp. J. 2015, 21, 201–206.
127. Huang, L.J.; Geng, L.; Peng, H.X. Microstructurally inhomogeneous composites: Is a homogeneous reinforcement distribution optimal? Prog. Mater. Sci. 2015, 71, 93–168.
128. Zhang, S.; Sun, D.; Fu, Y.; Du, H. Toughening of hard nanostructural thin films: A critical review. Surf. Coatings Technol. 2005, 198, 2–8.